

# The radio meteor signal path from transmitter to spectrogram: an overview

Tom Roelandts

Impulse Response, Beerse, Belgium  
tom@impulseresponse.eu

In this paper, we present an overview of the radio meteor signal path, from the sinusoidal carrier wave that is initially transmitted, to the spectrogram that is typically used as the final result in the receiving chain. We describe the amplitude modulation and Doppler shift that is caused by the meteor, the combination of the reflected with the directly received signal at the antenna, the down conversion in the receiver, the sampling, and the down sampling in software. A simulation of the complete process results in detailed plots at each of these steps.

## 1 Introduction

The results of the *Belgian Radio Meteor Stations (BRAMS)* network (Calders and Lamy, 2011), (Ranvier et al., 2015) are often analyzed through *spectrograms*. In this paper, we provide an overview of the complete radio meteor signal path that leads to these spectrograms at the very end of the receiving chain.

Starting from the knowledge that the transmitted signal is a simple sinusoidal carrier wave, the conceptual picture is clear. A BRAMS spectrogram represents the reflection of that carrier off a number of meteor trails, together with a relatively low amplitude directly received signal (and plane echoes, which we ignore in this paper). However, in practice, several things happen to the signal in addition to it being reflected off the meteor trail.

In this paper, we describe all the major effects that the signal encounters before it is finally plotted as a spectrogram. Additionally, we have implemented a simulation of the complete signal path, which allows showing detailed plots at each step. Both the description and the simulation are meant to demonstrate the major effects that happen, without necessarily capturing every last detail of each process.

## 2 Signal path

### Overview

Figure 1 shows an overview of the signal path. The initial carrier is modified by the interaction with the meteor trail, by being combined with the directly received signal at the antenna, by being down converted in the receiver, by being sampled, and by being down sampled in software. In the remainder of this paper, each of these steps is described in more detail.

The different effects are illustrated by plots that were generated through a simulation of the complete signal path. This simulation was performed at a radio frequency (RF) of 100 kHz. This is equivalent to using the true RF, since the down conversion step is independent of that RF.

### Transmitter

The transmitter produces a simple sinusoidal carrier wave at a frequency of  $f_T = 49970000$  Hz. Hence, the carrier wave can be defined as

$$\sin(2\pi f_T t),$$

where  $t$  is the time in seconds.

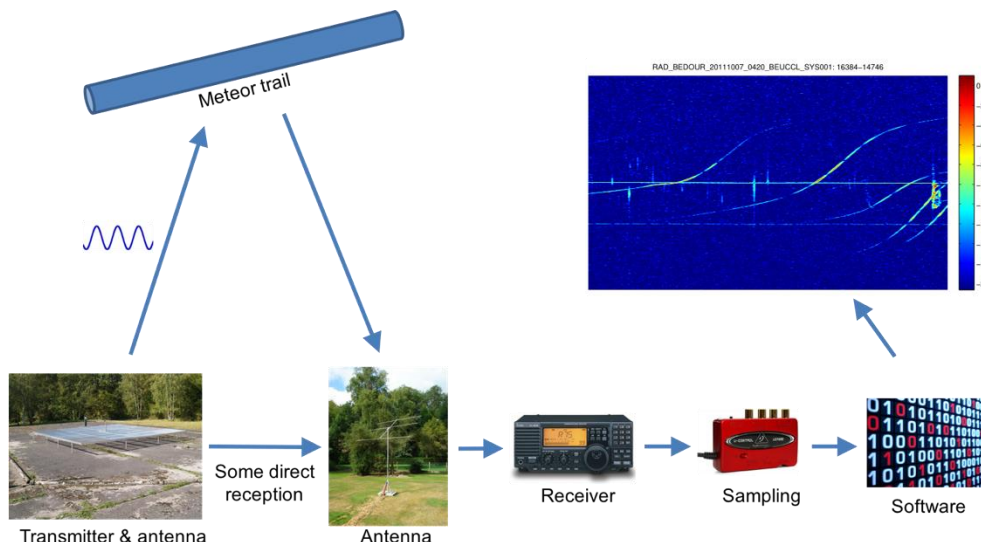


Figure 1 – Overview of the signal path.

### Meteor trail

If a meteor trail with a geometrically favorable orientation is present, it will reflect the carrier wave towards the antenna. The effect of this reflection is a modulation of the *amplitude* of the carrier. In the simulation, a simple meteor amplitude profile was used, consisting of a fast linear rise followed by an exponential decay (*Figure 2*). We write this amplitude profile as  $A(t)$ . The fast linear rise models the quick formation of the trail, while the exponential decay models its diffusion.

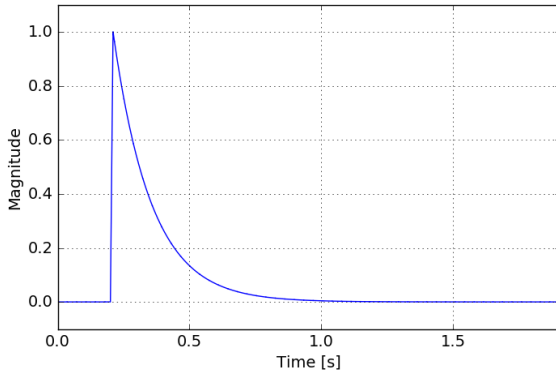


Figure 2 – Meteor amplitude profile.

In addition to the amplitude modulation, the reflection off the trail also causes a Doppler shift of the carrier frequency, if the trail is moving due to high altitude winds. Such a Doppler shift is observed very often in practice. If the reflection off the trail causes a Doppler shift of  $f_D$  Hz, then the received frequency will be  $f_T + f_D$  Hz.

Combining the amplitude profile of the meteor with the Doppler shift, the reflected wave that is received by the antenna is

$$A(t) \sin(2\pi(f_T + f_D)t).$$

This amplitude-modulated carrier is illustrated in *Figure 3*. The graph is solid blue because of the very high frequency of the carrier.

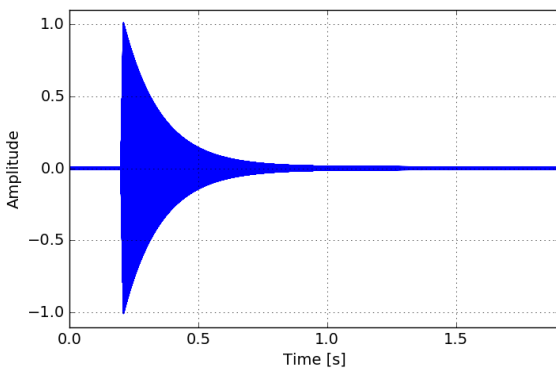


Figure 3 – Amplitude-modulated carrier after reflection off the meteor trail.

### Receiver Antenna

At most of the BRAMS stations, the antenna picks up a low-amplitude signal directly from the transmitter. When a meteor appears, its signal is combined with it. The directly received signal has a much lower amplitude than

many of the meteor reflections. However, this does not imply that it can be ignored. In the simulation, we have set the amplitude of the directly received signal to 1% of the maximum level of the simulated meteor.

Due to the Doppler shift that the reflected signal contains, the two signals that are combined at the antenna have a different frequency. At a direct reception level of  $D$ , the combined signal can be written as

$$D \sin(2\pi f_T t) + A(t) \sin(2\pi(f_T + f_D)t).$$

Summing two sinusoids with a slightly different frequency produces *beats*, which are variations in the amplitude of the signal due to alternating constructive and destructive interference. In the simulation, we have used a Doppler rate of 25 Hz. *Figure 4* shows how the resulting beats are superimposed on the received amplitude profile as small “bumps”. The frequency of 25 Hz can be recognized in the period of the amplitude variations.

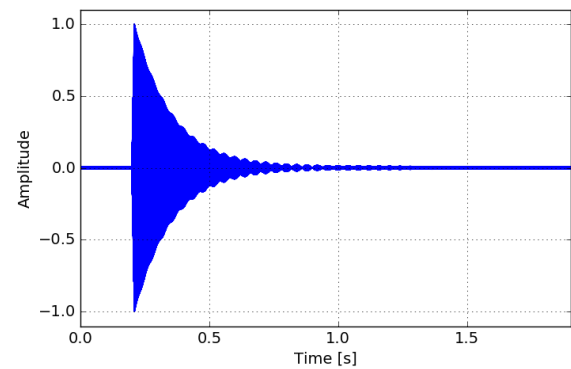


Figure 4 – The combined reflected and directly received signal at the antenna.

The corresponding power profile, which is simply the signal of *Figure 4* squared, is shown in *Figure 5*.

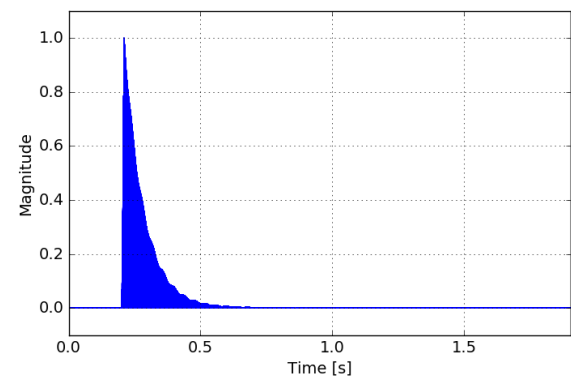


Figure 5 – Power profile of the received signal.

Although the Doppler shift of the reflection might be deduced from the period of these beats, it can easily be determined more directly from a spectrum or a spectrogram. Hence, it might be better to remove the directly received signal from the data, and avoid these beats altogether, since they might be obscuring the properties of the reflection itself. Removing the directly

received signal is relatively easy, since the received carrier is quite constant, both in frequency and in power.

### Receiver

The signal of *Figure 4* is the input to the receiver. This implies that the received spectrum can now be computed. *Figure 6* shows a part of the complete spectrum, centered at the original carrier frequency of, in the simulation, 100 kHz. There is a small peak at 100 kHz and the larger peak of the meteor reflection at an offset of 25 Hz (the Doppler offset).

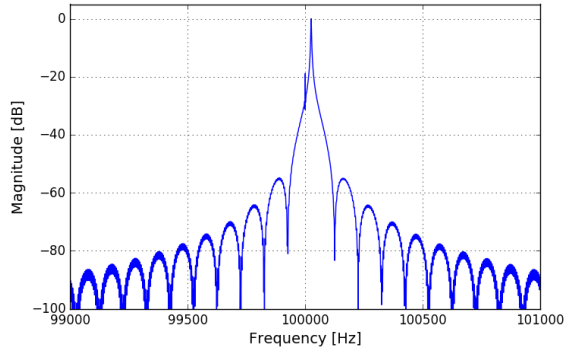


*Figure 6* – The spectrum that is received at the receiver.

At the receiver, this signal is *mixed*, i.e., *multiplied*, with a local oscillator (LO) at a small frequency offset of 1 kHz. This is done simply by tuning the receiver to a frequency of 49969000 Hz instead of the exact value of  $f_T$ . Note that this multiplication of signals is completely different from what happens at the antenna, where two signals are *added*. Moreover, the offset of the LO is on purpose. The effect of mixing the received signal with an LO that is offset is that the frequency contents of the meteor reflection is *down converted*, i.e., its frequencies are *shifted* from its original RF frequencies around  $f_T + f_D$  to a range of frequencies around 1 kHz.

When sinusoids at two frequencies  $f_1$  and  $f_2$  are multiplied, we have that

$$\sin(f_1) \sin(f_2) = \cos(f_1 - f_2) - \cos(f_1 + f_2),$$

from the well-known *product-to-sum* trigonometric identities. This means that, for an ideal mixer, the result of mixing is a first frequency component at the difference  $f_1 - f_2$  and a second frequency component at the sum  $f_1 + f_2$  of the original frequencies.

With the LO frequency  $f_{LO} = f_T - 1$  kHz, the two components of the directly received signal will be at  $f_T - f_{LO} = 1$  kHz and at  $f_T + f_{LO} = 2f_T - 1$  kHz. The two components of the meteor reflection, with its additional Doppler shift, will be at  $f_T + f_D - f_{LO} = f_D + 1$  kHz and at  $f_T + f_D + f_{LO} = 2f_T + f_D - 1$  kHz. The complete spectrum is shown in *Figure 7*. In that figure, there is clearly a first peak at 1 kHz and a second one just below 200 kHz (again, the simulation uses 100 kHz instead of  $f_T$ ). To illustrate that these peaks are indeed two copies of the original spectrum, compare the detailed

version of the spectrum that shows the component at 1 kHz (*Figure 8*) with *Figure 6*.

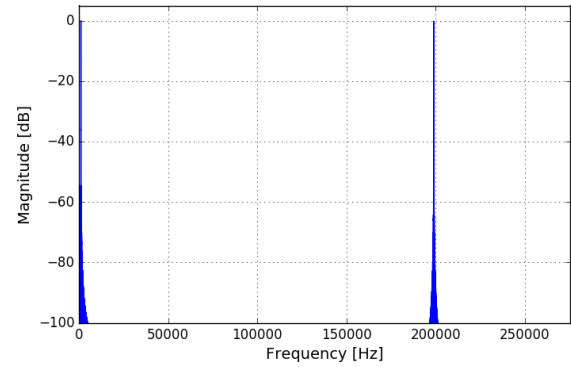


*Figure 7* – The full spectrum of the input signal mixed with the local oscillator.

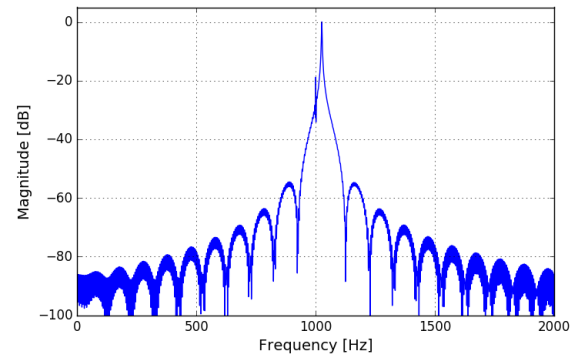


*Figure 8* – The spectrum of the input signal mixed with the local oscillator, centered at 1 kHz.

Because of this frequency shift, the signal can be sampled at much lower sampling rates than would be necessary to sample directly at the RF.

### Sampling

The Behringer UCA222 sampling device is programmed to sample the down converted signal at 22050 Hz. As is to be expected, the CODEC chip in the sampling device correctly low-pass filters the incoming signal, i.e., it removes frequencies above 11025 Hz, which is half the sampling rate (Texas Instruments, 2008).

The sampling process is the only place where the simulation is not exactly like the real setup. In the simulation, the complete signal path is digital, so there is no actual sampling step at this point. However, that step is replaced with a *down sampling* step that takes the sampling rate of the simulation, which is 551200 Hz, and reduces it to 5512 Hz. A proper low-pass filter with a cutoff frequency of 2756 Hz is included. The spectrum of the down sampled signal is shown in *Figure 9*.

### Software

The two operations in the software that are relevant for the signal path are a further down sampling from 22050 Hz to 5512 Hz and the generation of the spectrogram itself. For the down sampling, an additional low-pass filter is included, to remove the frequency contents between 11025 Hz to 2756 Hz. This makes the

output of the simulation equivalent to the output of the software.

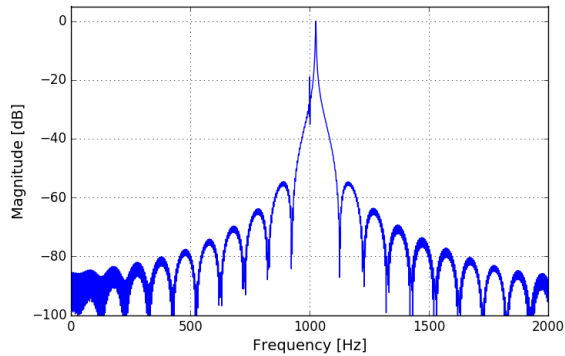


Figure 9 – Spectrum of the sampled signal.

### Comparison with the original spectrum

The spectrum at the final sampling rate of 5512 Hz (Figure 9) is very close to the originally received spectrum of Figure 8. Moreover, it is also quite close to the *bandpass* spectrum of Figure 6, confirming that down converting and down sampling the received signal is a valid methodology.

To further explore this, we can also compare the spectrum of Figure 9 with the spectrum of the original meteor profile. A *two-sided* spectrum, i.e., with 0 Hz in the middle, corresponding to the profile of Figure 2, is shown in Figure 10. Typically, a spectrum such as this would be shown *one-sided*, i.e., with a frequency range between 0 Hz and some appropriate maximum, since it is symmetrical. However, for easier comparison with the spectrum of Figure 9, we have chosen to plot it two-sided here.

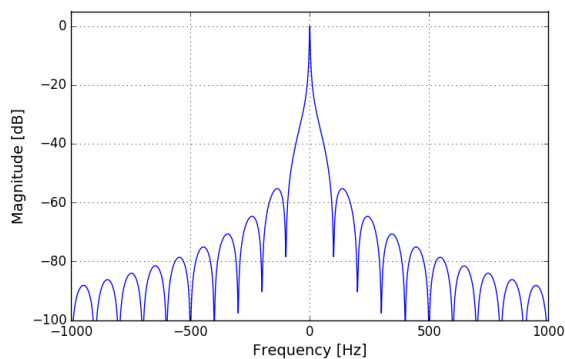


Figure 10 – Spectrum of meteor profile.

The main differences between Figure 9 and Figure 10 are the Doppler shift and the small secondary peak caused by the directly received carrier. However, apart from these small changes, both spectra are quite similar.

### Spectrogram

Although spectra are a very insightful way to compare the signal at the different stages of processing, they do not provide insight in the time component of the received signal. For that, a spectrogram is generated (Figure 11).

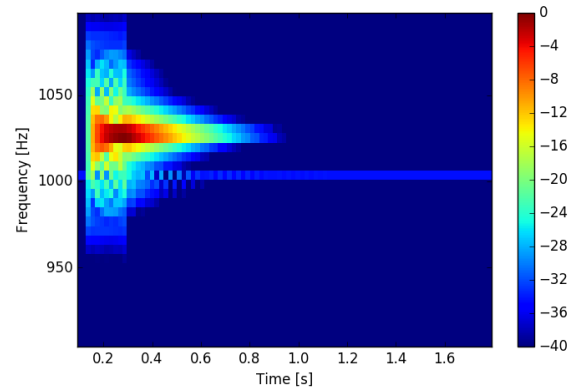


Figure 11 – Spectrogram of the sampled signal.

For comparison with the spectrograms as they are usually presented for BRAMS, Figure 12 shows the same spectrogram as Figure 11, but then for the usual time period of 5 minutes.

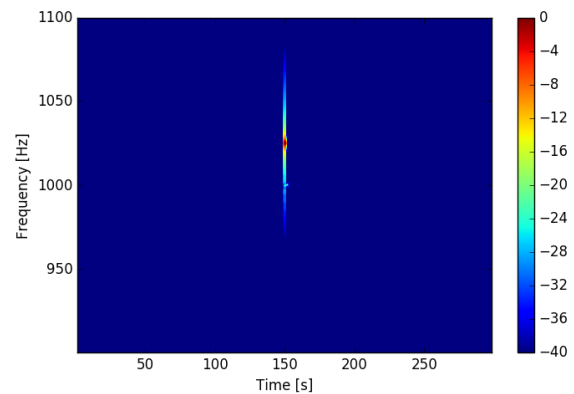


Figure 12 – Spectrogram of the sampled signal, rescaled to a time axis of 5 minutes.

The reflection in Figure 12 is close to a typical short meteor in an actual BRAMS spectrogram.

## 3 Conclusion

We have provided an overview of the complete signal path of a radio meteor, from the transmitter to the spectrogram as it is typically generated by a BRAMS station.

## References

- Calders S. and Lamy H. (2011). “Brams : status of the network and preliminary results”. In *Proceedings International Meteor Conference (IMC)*, Sibiu, Romania, pages 73–76.
- Ranvier S., Lamy H., Anciaux M., Calders S., Gamby E., De Keyser J. (2015). “Instrumentation of the Belgian Radio Meteor Stations (BRAMS)”. *International Conference on Electromagnetics in Advanced Applications (ICEAA)*, Turin, Italy, 7–11 September 2015, pages 1345–1348.
- Texas Instruments (2008). “PCM2902 Stereo Audio CODEC w/USB Interface” datasheet.